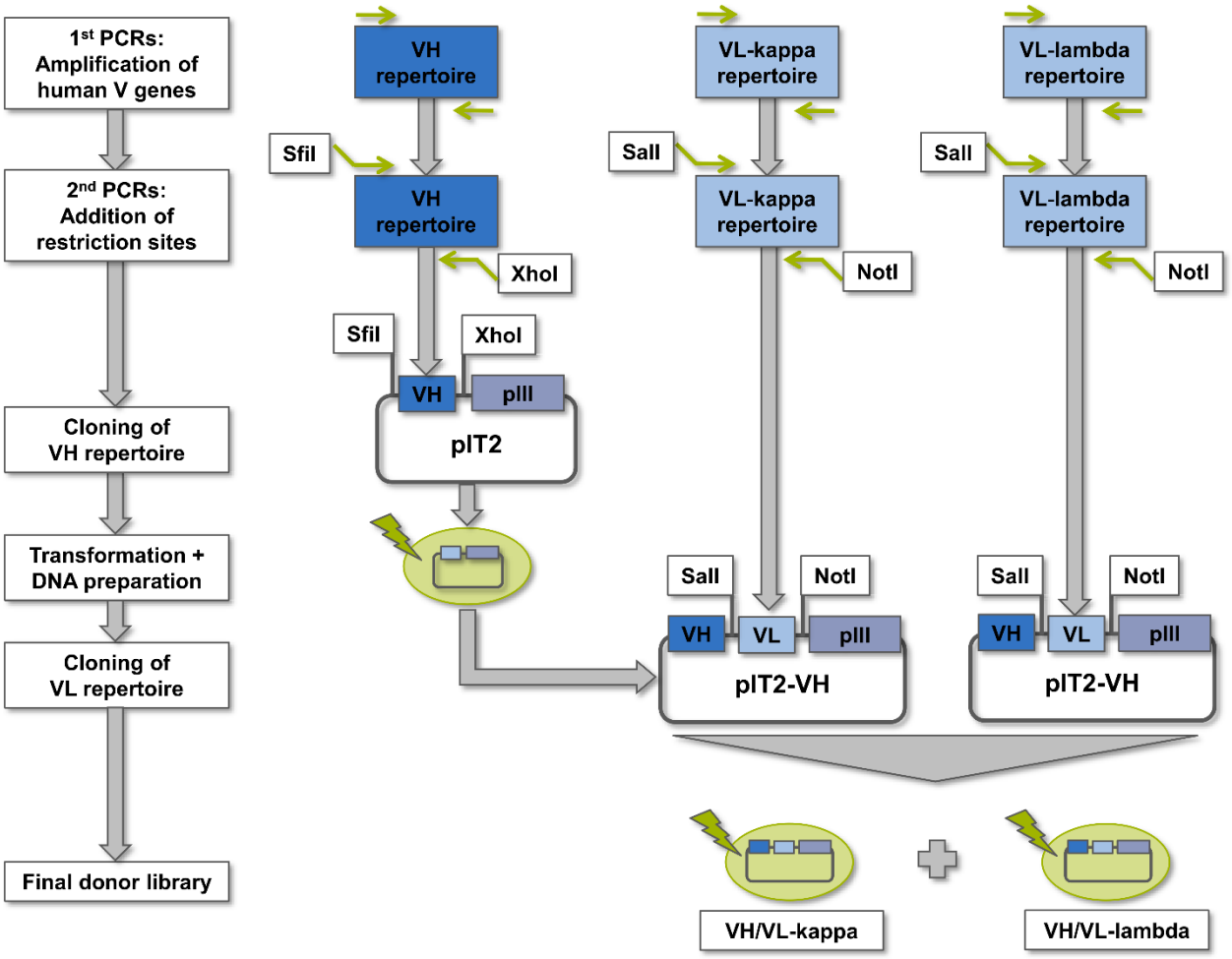

Supplemental Figure 1. Summary about WashU-1 phage display library. The human scFv antibody library was generated with a similar strategy used for cloning of LYNDAL (*13,14*). In brief, human antibody repertoires (IgG and IgM) were amplified by PCR from cDNA of mixed human spleen samples and cloned randomly into phagemid vector pIT2. This vector encodes for a 16 aa linker $(G_4S)_3T$ between the VH and VL domain of the scFv as well as adds an additional C-terminal 6xHis and Myc tag. First, the VH and VL repertoires were amplified in a first set of PCRs and completed by SfiI/XhoI (VH) or SalI/NotI (VL) restriction sites in a second set of PCRs. The VH repertories were cloned first by electroporation in *E. coli* TG1 (Lucigen, #60502), followed by cloning of the VL-kappa or VL-lambda repertories. WashU-1 possess a diversity of $3.3x10^8$ independent scFvs.

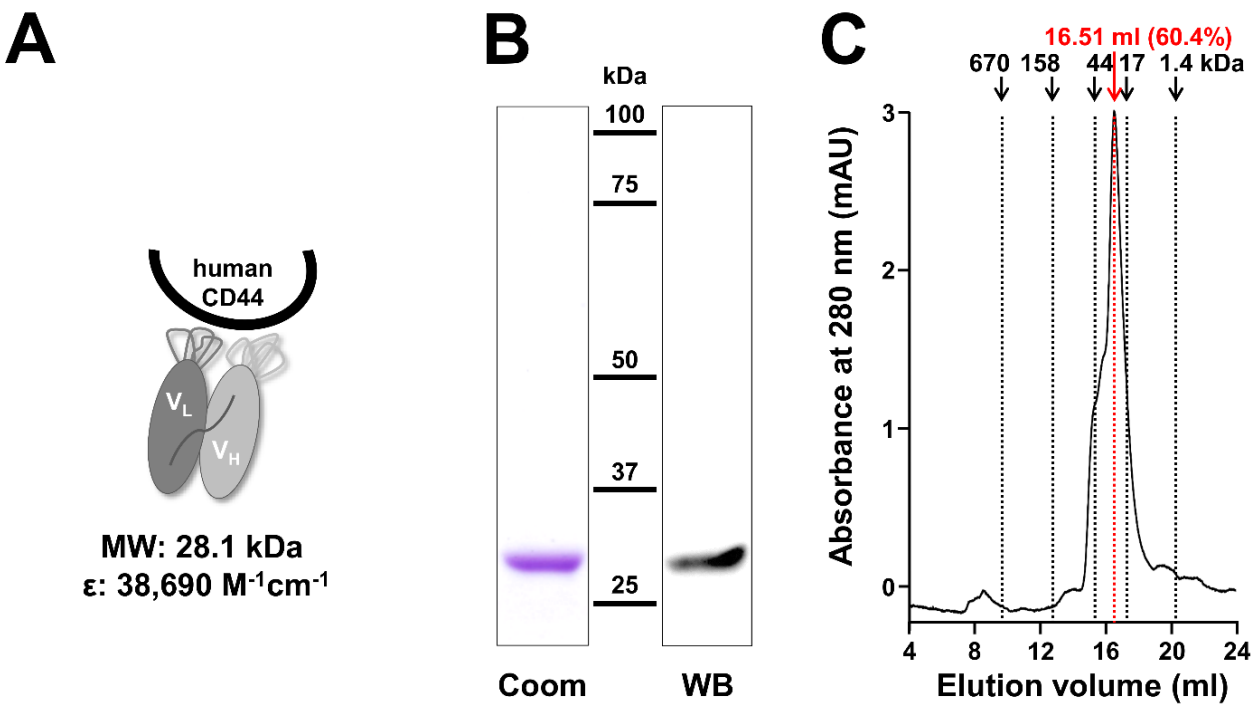

Supplemental Figure 2. Characterization of scFv-CD44. The antibody fragment was isolated from a human phage display library by 3 rounds of biopanning towards recombinant human CD44(Q21-E268) (Immune Technologies, #IT-300-001p). The phagmid vector containing the scFv-CD44 gene with C-terminal 6xHis and Myc tag was transformed into the amber codon non-suppressor *E. coli* strain Express I^q (NEB). ScFv-CD44 was solubility expressed and purified from the periplasmic fraction by IMAC as described before *(15)*. (A) ScFv-CD44 possessed VH-VL orientation connected by a flexible 16 aa peptide linker. Based on the scFv-CD44 sequence, the theoretical molecular weight (MW) was calculated to be 28.1 kDa with an extinction coefficient (ε) of 38,690 $M^{-1}cm^{-1}$. (B) Characterization by Coomassie (Coom) stained gradient SDS-PAGE (3 µg/lane) of the reduced scFv-CD44 revealed high purity (>98%) with a single dominant band running at the expected MW. The integrity was analyzed by WB using a primary mouse anti-His monoclonal antibody (mAb) (Santa Cruz Biotechnology, #sc-8036) and a secondary goat anti-mouse polyclonal antibody (pAb) peroxidase conjugate (Jackson ImmunoResearch, #115-035-008) showing no obvious degradation products. (C) Analysis of the oligomeric state of scFv-CD44 (31 µg) by FPLC showed a main peak of monomeric product (60.4% at 16.5 ml) and slight formation of a dimeric fraction (8.9% at 15.4 ml).

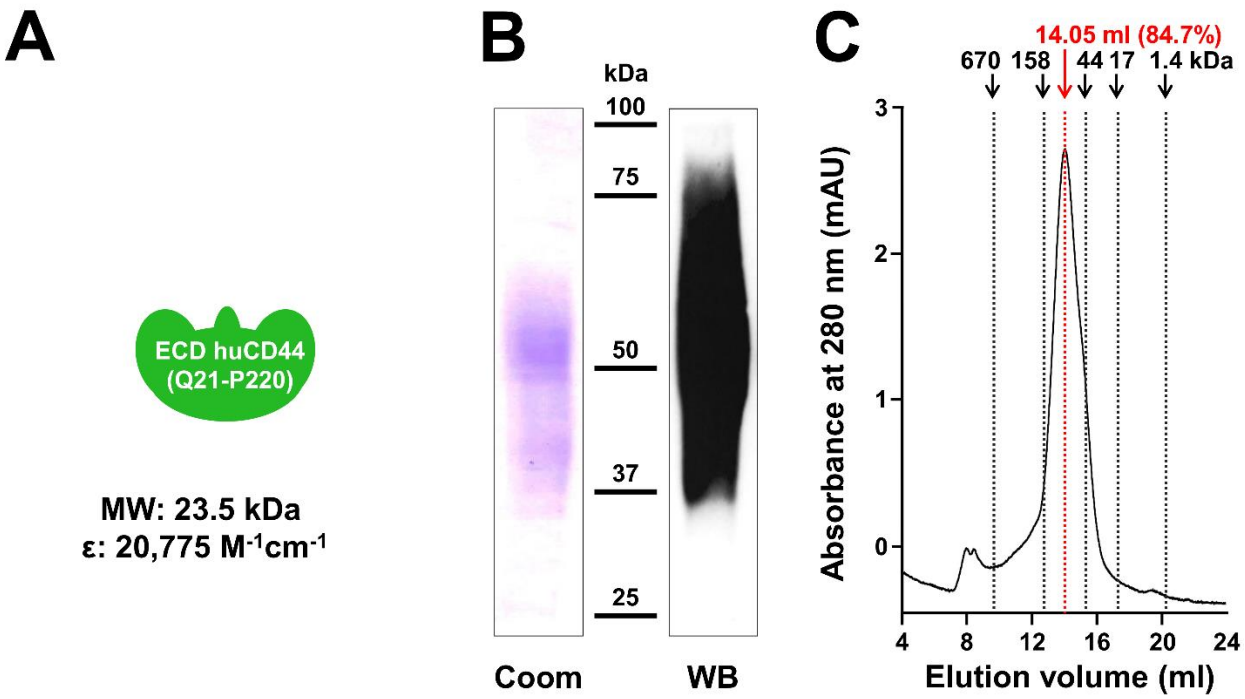

Supplemental Figure 3. Characterization of recombinant human CD44. *De novo* synthesized DNA encoding for the ECD of human CD44(Q21-P220) was amplified by PCR and cloned into pTT28, a derivative of the pTT vector (National Research Council of Canada). The gene was cloned via restriction enzymes NheI and AgeI to add a C-terminal 8xHis tag. Endo-free plasmid DNA was transiently transfected into HEK293-6E cells and purified after five days expression from supernatant via IMAC purification. (A) Based on the amino acid (aa) sequence, the theoretical MW was calculated to be 23.5 kDa with an extinction coefficient (ε) of 20,775 M-1cm-1. (B) Characterization by Coomassie-stained gradient SDS-PAGE (10 µg/lane) of the reduced protein revealed high purity (>98%) with a broad band spanning from about 35 kDa up to 100 kDa due to the highly glycosylated nature of the mammalian cell produced protein. The integrity was confirmed by WB using a primary mouse anti-His mAb (Santa Cruz Biotechnology, #sc-8036) and secondary goat anti-mouse pAb peroxidase conjugate (Jackson ImmunoResearch, #115-035-008). (C) Analysis of the oligomeric state of recombinant CD44 proteins (56 µg) by FPLC revealed a broad main peak of monomeric product (84.7% at 14.1 ml).

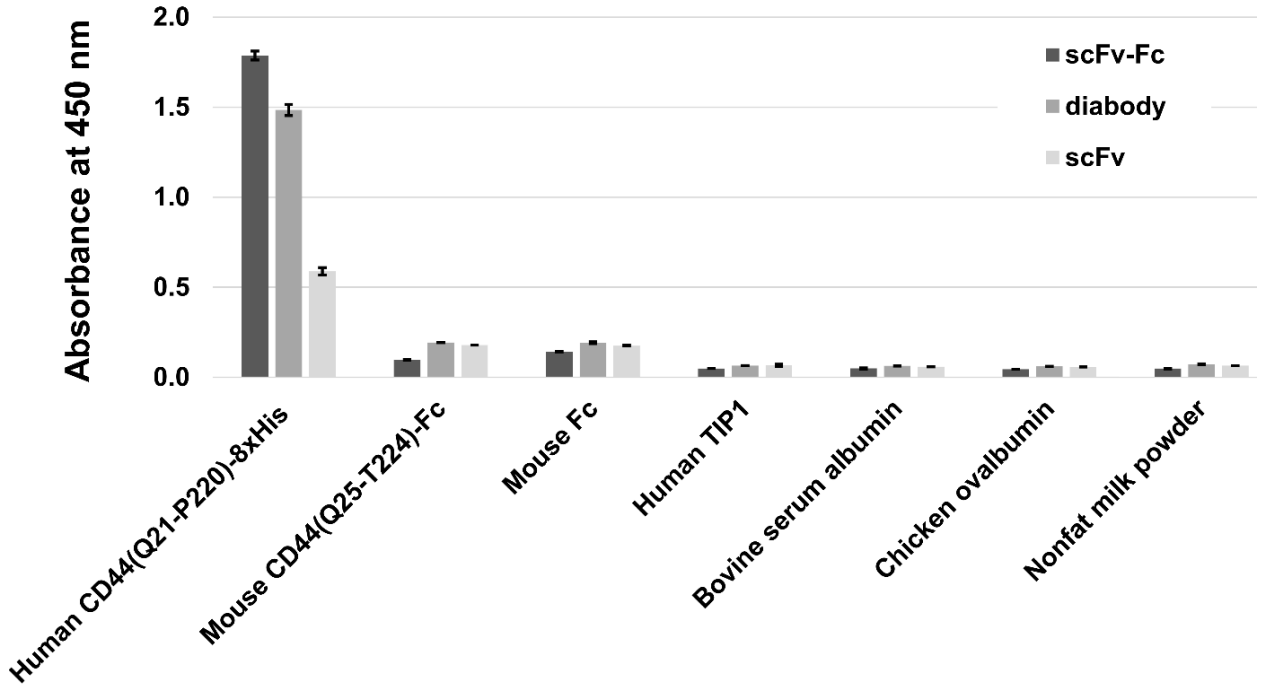

Supplemental Figure 4. Specificity and cross-reactivity analysis of the antibody lead towards human and murine CD44, and a panel of irrelevant proteins by ELISA. Proteins were diluted in PBS and coated with 3 µg/ml (milk powder: 20 mg/ml) overnight at 4°C on an ELISA plate (100 µl/well). The milk-blocked plate was incubated with the antibody in different recombinant formats (i.e., scFv, diabody, and scFv-Fc) with 1 µM in 2% MPBS for 2 hours at room temperature (RT). The scFv-CD44 (monovalent) and diabody-CD44 (bivalent) were expressed in periplasm of *E.coli* and purified via IMAC purification (all >98% pure). The bivalent scFv-Fc-CD44 was expressed by transiently transfected HEK293-6E cells and purified by protein G purification (>98% pure). Both the scFv-CD44 and the diabody-CD44 were detected via their C-terminal Myc tag using a primary mouse mAb 9E10 (7.5 µg/ml) and secondary goat anti-mouse pAb, $F(ab')_2$-specific peroxidase conjugate (Jackson ImmunoResearch, #115-035-072). The scFv-Fc-CD44 was detected via a goat anti-human pAb peroxidase conjugate (Jackson ImmunoResearch, #109-035-098, minimal cross-reactivity to mouse serum) using TMB substrate and 2 M sulfuric acid as stop solution. Absorbance was measured in a microplate reader at 450 nm. Data are represented as the mean of triplicates ±SE.

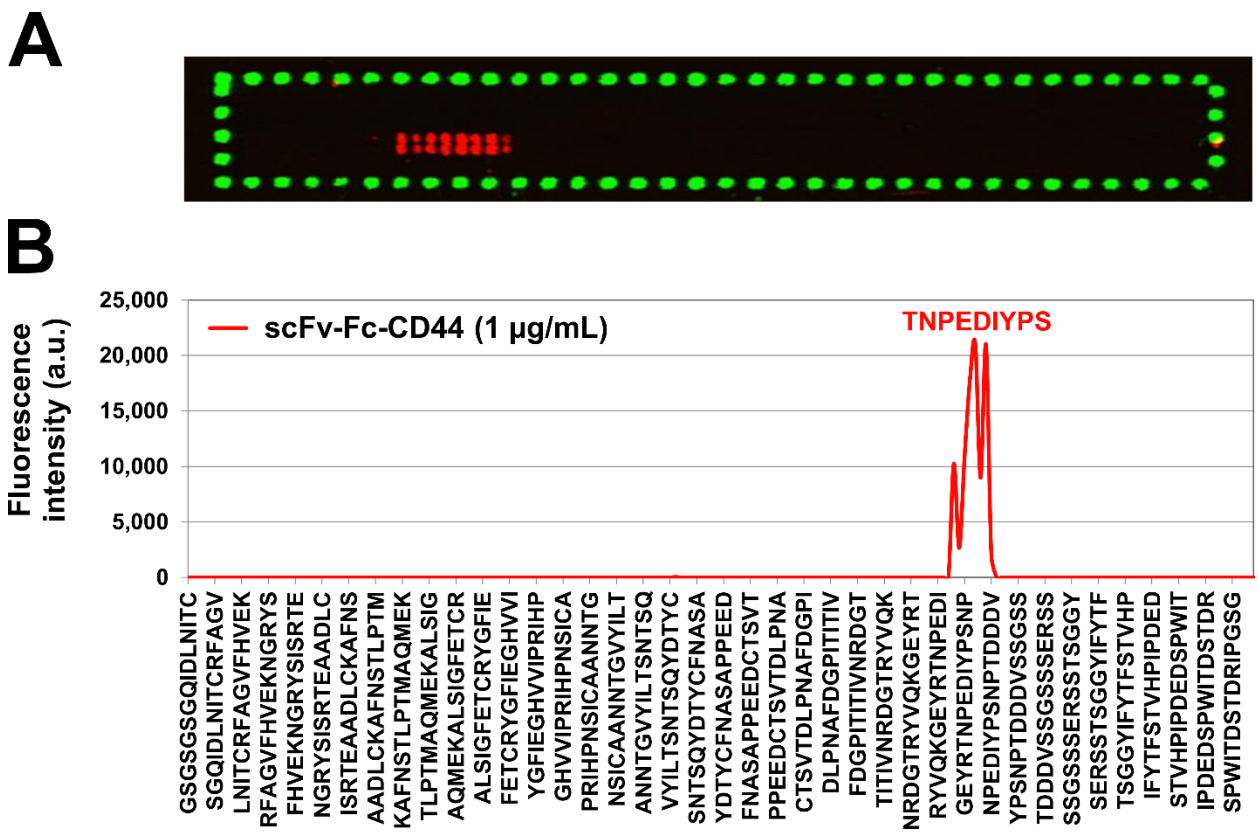

Supplemental Figure 5. Epitope mapping of the antibody lead by PEPperMAP technology. The human CD44(Q21-P220) aa sequence (UniProtKB: P16070) was translated into linear overlapping 15 peptides with a 14 aa overlap and elongated with neutral GSGSGSG linkers at the C- and N-terminus. The resulting CD44 peptide microarrays contained 200 different peptides printed in duplicate and were framed by additional hemaglutinin (YPYDVPDYAG, 76 spots) control peptides. The microarray was incubated with scFv-Fc-CD44 in incubation buffer (PBS, pH 7.4 with 0.05% Tween 20 and 10% blocking buffer (Rockland), followed by staining with a secondary goat anti-human IgG (Fc) DyLight680 conjugate. A mouse anti-hemaglutinin mAb (12CA5) DyLight800 conjugate served as control. A LI-COR Odyssey Imaging System was used for the read-out of the fluorescence intensity (arbitrary unit, a.u.) at a scanning intensity of 7/7 (red/green). Quantification of the spot intensities and peptide annotation were done with PepSlide Analyzer. (A) Positive signals (red) with high signal-to-noise ratios were observed for 8 adjacent peptides with well-defined staining of the control peptides (green). The strong response against a single epitope-like spot pattern formed by adjacent peptides suggest a consensus motif TNPEDIYPS as linear epitope of the lead antibody.

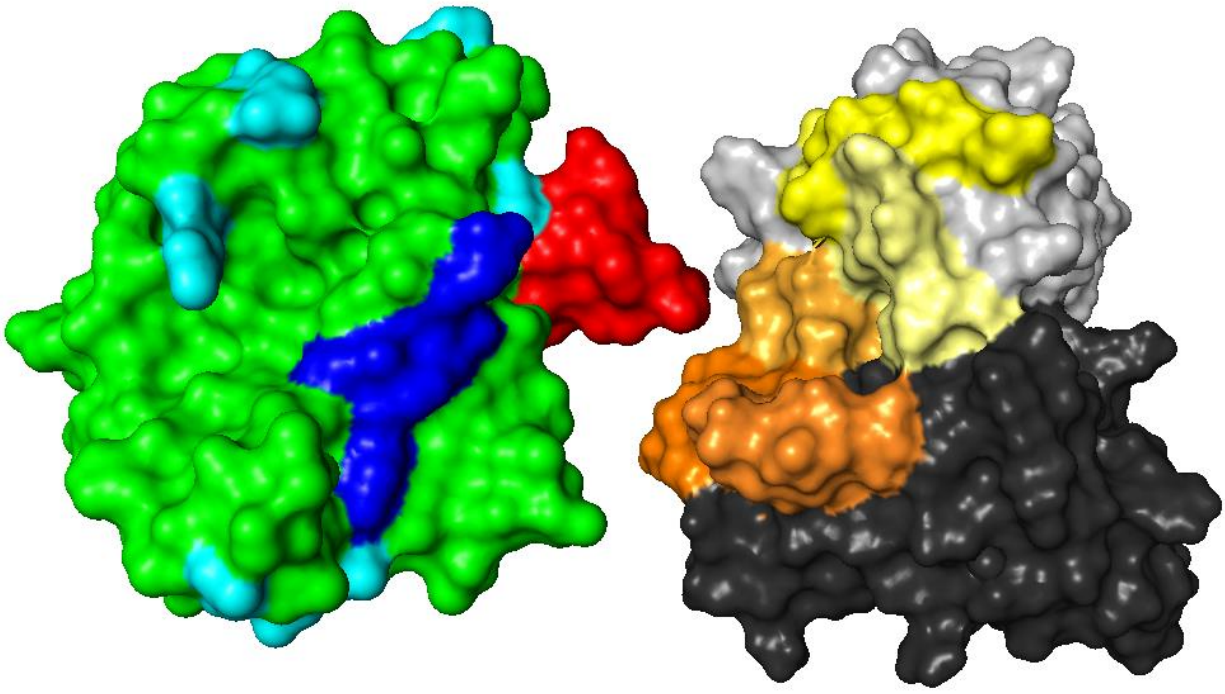

Supplemental Figure 6. Structural representation of human CD44 (left) and scFv-CD44 (right). A high-resolution (1.6 Å) crystal structure (PDB file: 4PZ4) of the ECD of human CD44(Q21-S171) is shown on the left in green. CD44 possess two putative HA binding domains within the distal ECD that are rich on basic amino acids. The major HA bindig site is situated near the NH_2 terminus as highlighted in dark blue (R41, Y42, R78, and Y79). The second HA binding site is located more membrane proximal as shown in bright blue (N100, N101, R150, R154, K158, and R162). The putative linear epitope of the lead antibody is depicted in red (T163-S171). The scFv-CD44 structure was modeled by the ROSIE Rosetta Online Server based on its VH and VL aa sequence and the CDRH3 loop with the highest obtained score. The framework regions of the VH domain is shown in black with the different CDR regions in orange. The framework regions of the VL domain is depicted in grey and the corresponding CDRs in yellow. The CDRs of the variable domains form a pocket enclosing the finger-like epitope of human CD44. The structures were visualized with PyMOL molecular graphics system, version 2.3.0 (Schrödinger).

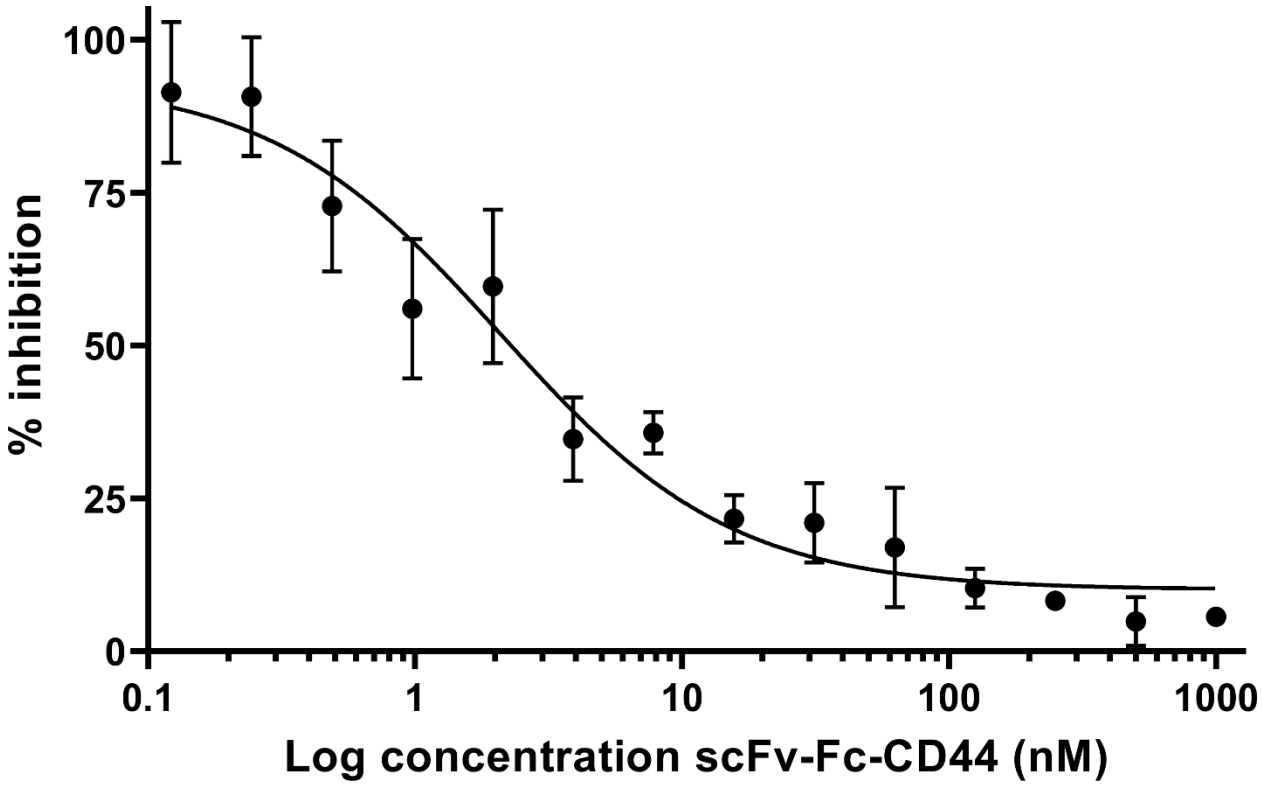

Supplemental Figure 7. ScFv-Fc-CD44 efficiently blocks the binding of HA to recombinant human CD44 in concentration dependent manner. One µg/ml of recombinant human CD44(Q21-E268) (Immune Technologies, #IT-300-001p) was coated overnight in PBS at 4 ºC on an ELISA plate (100 µl/well). After blocking (1 hour with 2% BSA in PBS), 0.1 µg/well of HA-biotin (Sigma-Aldrich, #B1557) and different concentration of the scFv-Fc-CD44 was incubated at RT for 1 hour. Detection of the HA-biotin binding to recombinant CD44 was performed by high sensitivity streptavidin-HRP (Thermo Fisher Scientific, #21130) using TMB solution and 2 M sulfuric acid as stop solution. Absorbance was read at 450 nm in a BioTek ELx800 microplate reader. The IC_{50} for blocking the binding of HA-biotin to human CD44(Q21-E268) by the scFv-Fc-CD44 was 2.1 nM (R^2=0.9230). Absorbance data (triplicates, minus background) were normalized and the IC_{50} calculated based on nonlinear regression analysis in GraphPad Prism 8 using log(inhibitor) vs. response (three parameters).

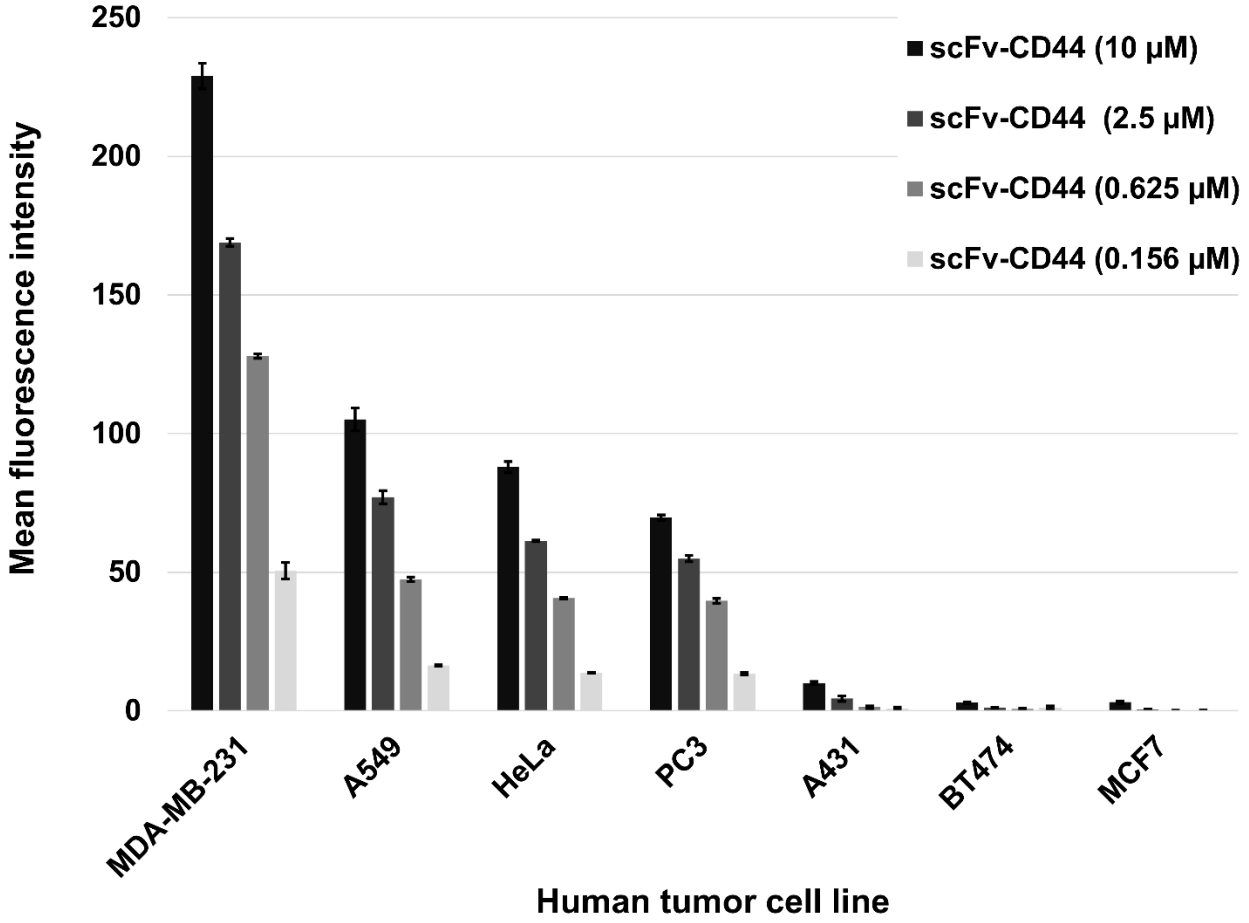

Supplemental Figure 8. ScFv-CD44 specifically binds to human tumor cell lines expressing different levels of CD44. The scFv-CD44 showed a similar concentration-dependent pattern of fluorescence signals in flow cytometry when compared to a CD44-specific mouse mAb clone B-F24 (Abcam, #ab27284) (data not shown). The scFv-CD44 was diluted in flow buffer (2% FBS in PBS) and incubated with $0.3x10^6$ cells/well (2 hours at RT). Detection of scFv-CD44 was performed via the C-terminal Myc tag using murine mAb 9E10 (7.5 µg/ml) and secondary goat anti-mouse pAb fluorescein isothiocyanate conjugate (Jackson ImmunoResearch, #115-095-008). The positive control was detected via the same secondary goat anti-mouse pAb fluorescein isothiocyanate conjugate. Mean fluorescence intensities of cells were analyzed in duplicates in a MACSQuant Analyzer 10 (Miltenyi Biotec) using the MACSQuantify Software. Data are represented as the mean of duplicates ±SE.

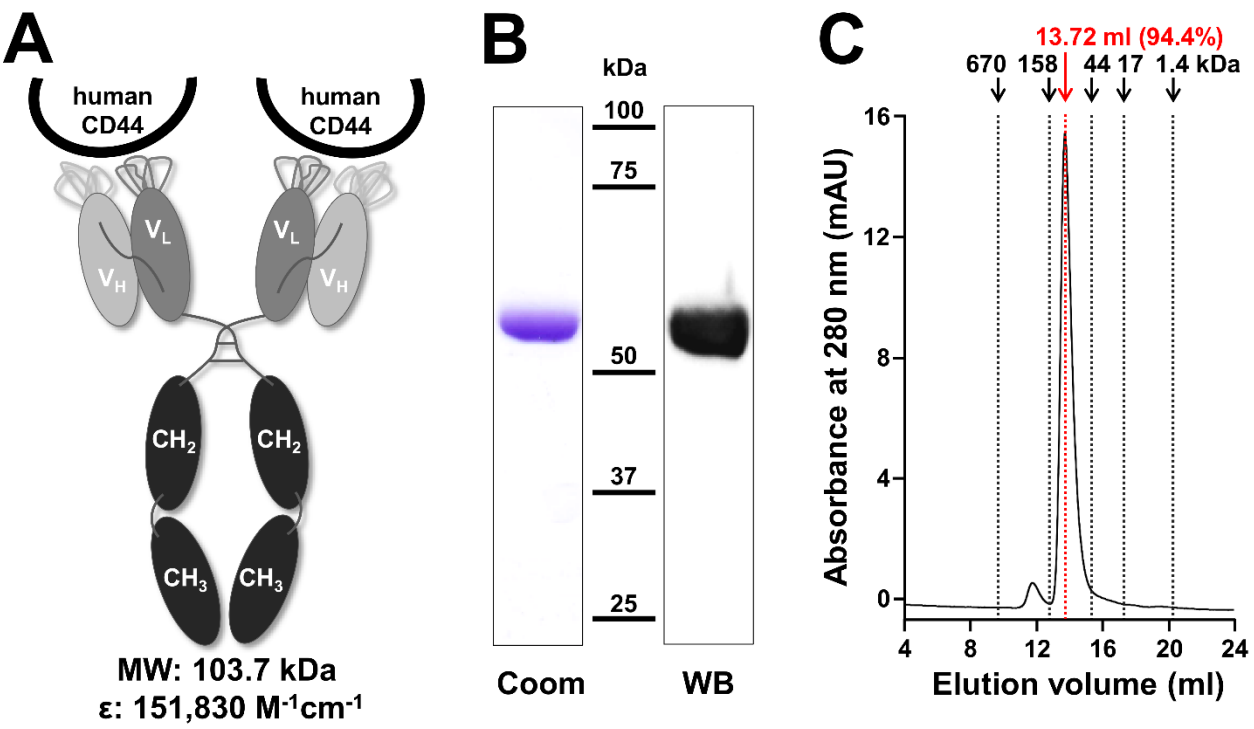

Supplemental Figure 9. Characterization of scFv-Fc-CD44. The scFv-CD44 gene was amplified by PCR with scFv-specific primers to add NarI and EcoRV restriction sites and cloned into vector pYD11 (National Research Council of Canada) adding an intrinsic human IgG_1 Fc part at the C-terminus. Plasmid DNA was transiently transfected into HEK293-6E cells and purified after five days of expression from supernatant via IMAC purification. (A) Based on the aa sequence, the theoretical MW was calculated to be 103.7 kDa with an extinction coefficient (ε) of 151,830 $M^{-1}cm^{-1}$ for the native scFv-Fc-CD44. (B) Characterization by Coomassie-stained gradient SDS-PAGE (5 µg/lane) of the reduced protein revealed high purity (>98 %) with a distinct band for a reduced single-chain (theoretical MW: 51.9 kDa). The integrity was confirmed by WB using a goat anti-human pAb peroxidase conjugate (Jackson ImmunoResearch, #109-035-098). (C) Analysis of the oligomeric state of scFv-Fc-CD44 (45 µg) by FPLC revealed a broad main peak of monomeric product (94.4% at 13.7 ml). (D)

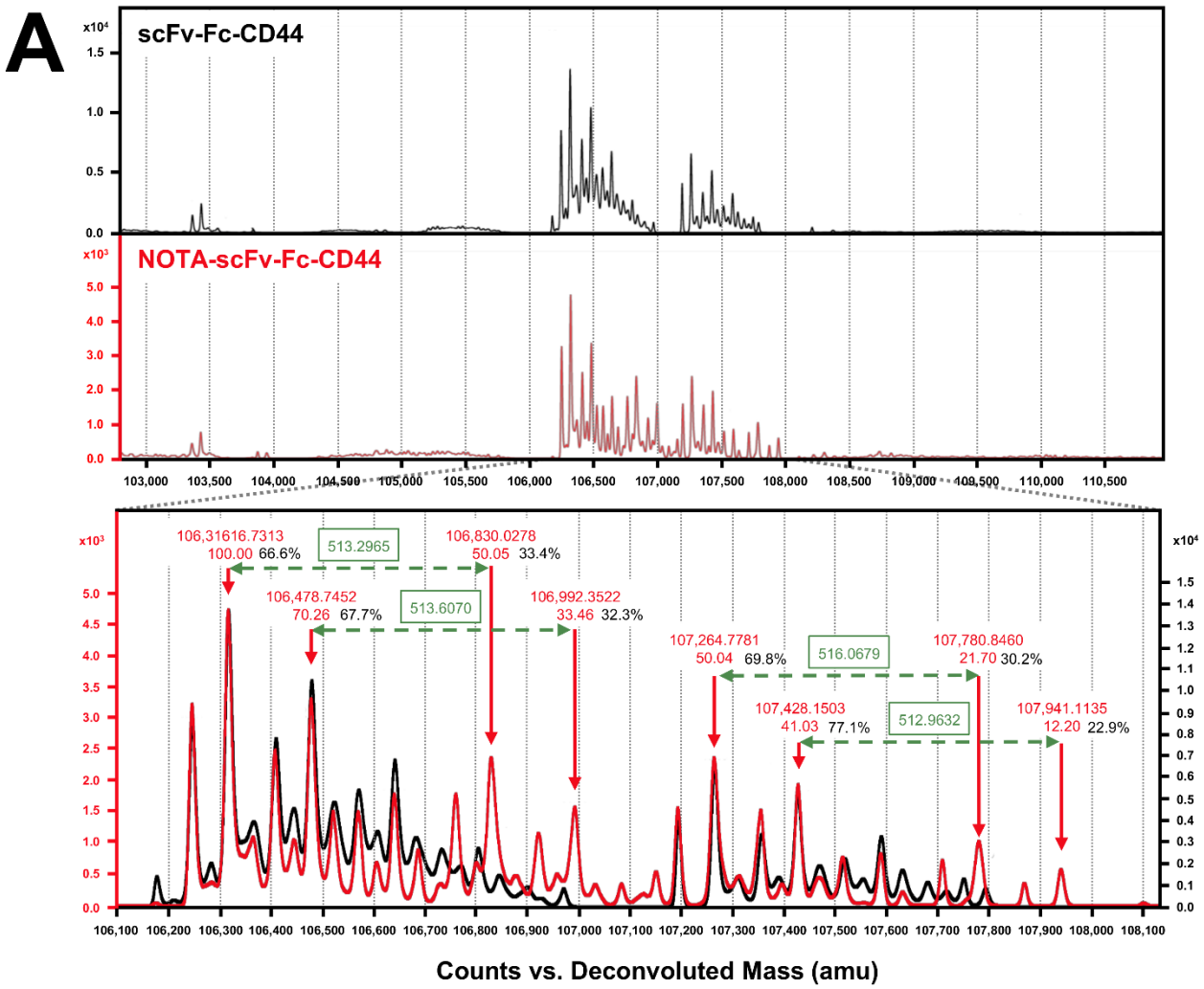
A
scFv-Fc-CD44
NOTA-scFv-Fc-CD44
106,31616.7313
100.00 66.6%
513.2965
106,830.0278
50.05 33.4%
106,478.7452
70.26 67.7%
513.6070
106,992.3522
33.46 32.3%
107,264.7781
50.04 69.8%
516.0679
107,780.8460
21.70 30.2%
107,428.1503
41.03 77.1%
512.9632
107,941.1135
12.20 22.9%
Counts vs. Deconvoluted Mass (amu)

B

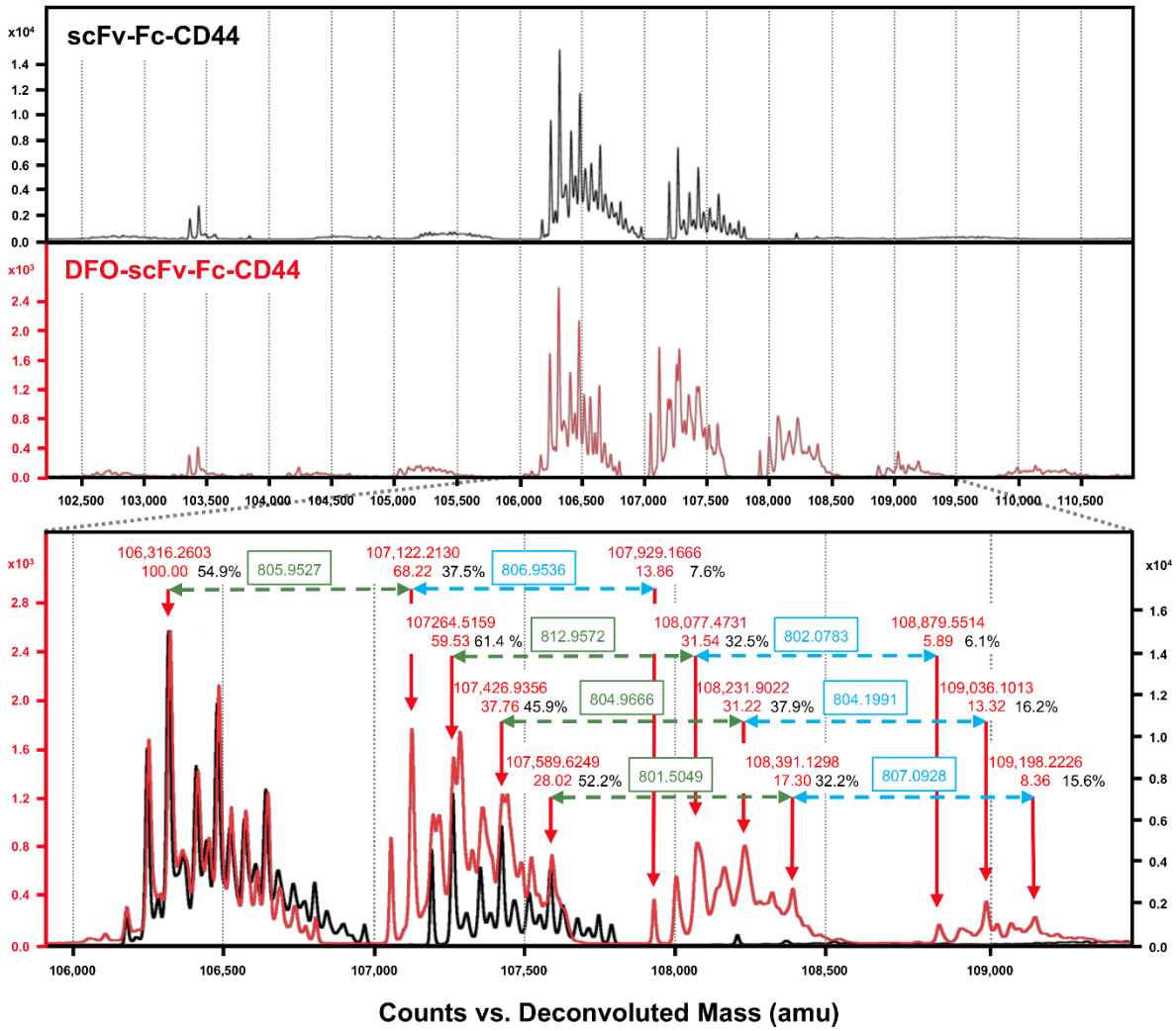
scFv-Fc-CD44
DFO-scFv-Fc-CD44
106,316.2603
100.00 54.9%
805.9527
107,122.2130
68.22 37.5%
806.9536
107,929.1666
13.86 7.6%
107264.5159
59.53 61.4 %
812.9572
108,077.4731
31.54 32.5%
802.0783
108,879.5514
5.89 6.1%
107,426.9356
37.76 45.9%
804.9666
108,231.9022
31.22 37.9%
804.1991
109,036.1013
13.32 16.2%
107,589.6249
28.02 52.2%
801.5049
108,391.1298
17.30 32.2%
807.0928
109,198.2226
8.36 15.6%
Counts vs. Deconvoluted Mass (amu)

Supplemental Figure 10. Analysis of chelated scFv-Fc-CD44 by mass spectrometry. Intact mass of the unconjugated (black curves), or conjugated scFv-Fc (red curves) were analyzed by high-resolution QTOF (Quadrupole Time-of-Flight) LC/MS (Liquid Chromatography/Mass Spectrometry). Samples were concentrated by Amicon Ultra-0.5 centrifugal filters to exchange buffer to 200 mM ammonium acetate buffer (pH 6.9) by centrifugation (10x times) to about 20 µM. Frozen samples were thawed on ice and diluted to 2 pmol/µl in 0.1% formic acid. Two ul of centrifuged supernatants injected via an autosampler and run on a fused silica column packed with Magic C8 (3.5 µm particles, 100Å) linked to a C8 Captrap column (both Michrom Bioresources) by elution with a 30 min gradient of acetonitrile. Data were acquired on a calibrated Agilent 6520 QTOF and examined using the Qualitative Analysis software provided with the instrument. The maximum entropy was used to deconvolute multi-charge-state peaks to intact mass using the protein deconvolution model. The unconjugated scFv-Fc-CD44 (black, top profiles) shows a main peak at about 106.3 kDa and several additional peaks presumably representing different states of glycosylation. NOTA-conjugated (A) or DFO-conjugated (B) profiles (red, middle profiles) show additional peaks for the conjugated products. The zoomed in overlays (bottom profiles) revealed the additional peaks of the conjugated samples with a mean calculated mass of 513.9837±0.7071 for NOTA and 804.7126 ±1.4531 for DFO. Based on the relative peak heights of the conjugated samples, the average number of NOTA or DFO per scFv-Fc-CD44 was 0.30±0.02 and 0.58±0.06, respectively. The ratio of unconjugated to conjugated species was 1/0.42 (scFv-Fc-CD44/NOTA-scFv-Fc-CD44) and 1/0.65/0.21 (scFv-Fc-CD44/DFO-scFv-Fc-CD44/DFO-DFO-scFv-Fc-CD44).

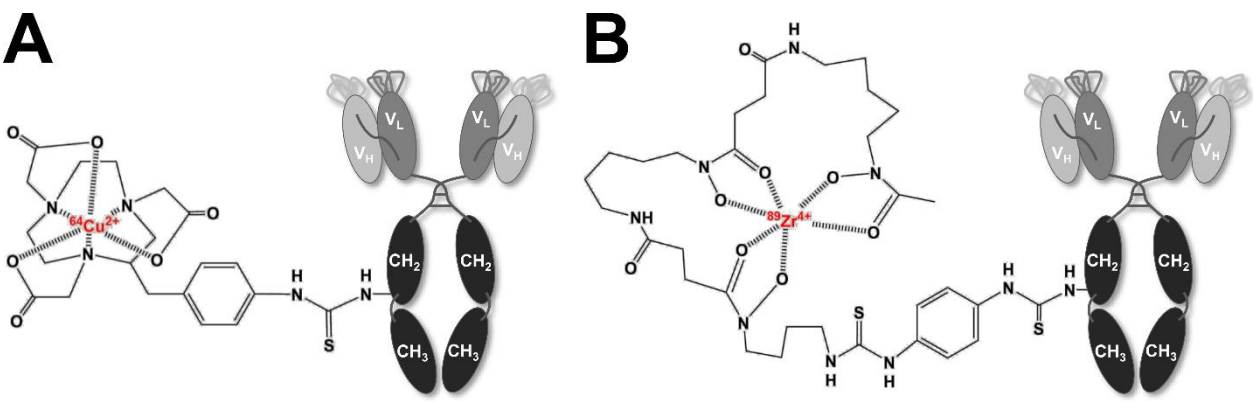

Supplemental Figure 11. Schematic representation of scFv-Fc-CD44 modified with chelator p-SCN-Bn-NOTA (A) and p-SCN-Bn-DFO (B) and labeled with either ^{64}Cu (A) or ^{89}Zr (B). Frozen aliquots of the scFv-Fc-CD44 (1-2 mg/ml) were dialyzed against 0.1 M carbonate buffer (pH 9.0) and conjugated via its primary amines with chelator (both Macrocyclics, 2 mM in DMSO) p-SCN-Bn-NOTA (#B605) or p-SCN-Bn-DFO (#B705) in a molar ratio of 1 (scFv-Fc) to 5 (chelator) for 1 hour at 37°C while gently rocking at 40 rpm. Buffer-exchanged conjugates NOTA-scFv-Fc-CD44 (0.1 M NH_4OAc pH 6.0) and DFO-scFv-Fc-CD44 (1 M HEPES, pH 7.2) were kept frozen until labeling with ^{64}Cu ($^{64}CuCl_2$ diluted in 0.1 M NH_4OAc, pH 6.0) or neutralized (pH 6.8-7.4) ^{89}Zr solution (^{89}Zr-oxalate diluted in 1 M HEPES, pH 7.2) for 1 hour at 37°C (300 rpm) using about 18.5 MBq (500 µCi) for 200 µg of scFv-Fc. To complex unreacted radiometals, chelex-treated 50 mM DTPA solution (pH 7.0) was added (1/10 of total volume) and incubated for further 5 min at 37°C (300 rpm). Final products were obtained by buffer exchange with PBS (pH 7.2) via Zeba spin columns (Thermo Fisher Scientific). The radiochemical purity of the products was confirmed by ITLC as described before (*16*). ^{64}Cu ($t_{1/2}$=12.7 h, β^+=17%, β^-=39%, EC=43%, E_{max}=0.656 MeV) was produced by a (p,n) reaction on enriched ^{64}Ni on a TR-19 biomedical cyclotron (Advanced Cyclotron Systems) at Washington University Cyclotron Facility and purified with an automated system by standard procedures (*17*). ^{89}Zr ($t_{1/2}$=78.4 h, EC=76.6 %, β+=22.3%, $E_{ave.}$(β+)=396.9 keV, $R_{ave.}$(β+)=1.18 mm) was produced via the ^{89}Y(p,n)^{89}Zr transmutation reaction on a CS-15 cyclotron (Cyclotron Corporation) at Washington University Cyclotron Facility and purified with an automated module by standard procedures (*18*).

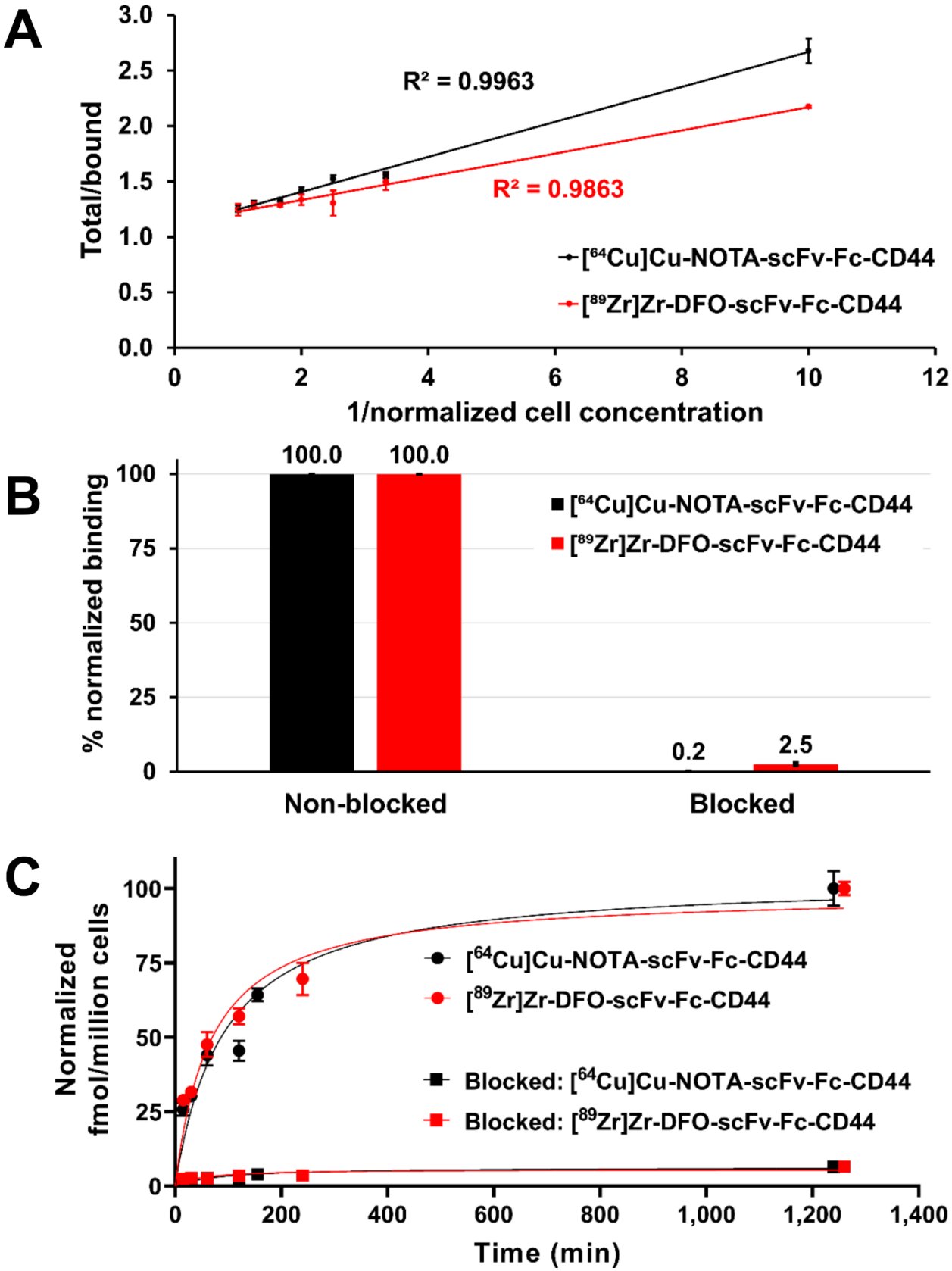
A
Total/bound
1/normalized cell concentration
R² = 0.9963
R² = 0.9863
[64Cu]Cu-NOTA-scFv-Fc-CD44
[89Zr]Zr-DFO-scFv-Fc-CD44
B
% normalized binding
100.0
100.0
0.2
2.5
Non-blocked
Blocked
[64Cu]Cu-NOTA-scFv-Fc-CD44
[89Zr]Zr-DFO-scFv-Fc-CD44
C
Normalized fmol/million cells
Time (min)
[64Cu]Cu-NOTA-scFv-Fc-CD44
[89Zr]Zr-DFO-scFv-Fc-CD44
Blocked: [64Cu]Cu-NOTA-scFv-Fc-CD44
Blocked: [89Zr]Zr-DFO-scFv-Fc-CD44

Supplemental Figure 12. (A) Cell binding studies. Representative plot of activity (total/bound) versus 1/[normalized cell concentration] used to calculate the immunoreactive fraction of [^{64}Cu]Cu-NOTA-scFv-Fc-CD44 (black) and [^{89}Zr]Zr-DFO-scFv-Fc-CD44 (red) in MDA-MB-231 cells. (B) Fifteen µg of native scFv-Fc-CD44 was used to specifically block the binding of the radiolabeled scFv-Fcs to 2.5x10^6 MDA-MB-231 cells/well. (C) Representative internalization assays of the radiolabeled scFv-Fcs-CD44 into MDA-MB-231 cells. Data are presented as triplicates of mean ±SE. The immunoreactivity towards binding to CD44+ MDA-MB-231 cells was done by Lindmo assay (*19*). Five thousand cpm (50 µl) were added to MDA-MB-231 cells in increasing concentrations (0.25 to 2.5x10^6 cells/500 µl PBS) in triplicate for 1 hour at RT. Pelleted cells were washed twice with PBS, and counted for ^{64}Cu or ^{89}Zr activity. The specific binding was calculated as the ratio of bound radioactivity to the total amount of administered activity after background correction. To determine the blocking efficiency, 15 µg of the non-radiolabeled scFv-Fc lead was added to 2.5x10^6 of MDA-MB-231 cells/well in triplicate and the ratio of blocked to non-blocked activity calculated. Internalization was performed as described before (*20*) using 5x10^5 of MDA-MB-231 cells/well. Here, CD44-specific blocking agent (15 µg scFv-Fc-CD44) was added in triplicate, followed by addition of either [^{64}Cu]Cu-NOTA-scFv-Fc-CD44 or [^{89}Zr]Zr-DFO-scFv-Fc-CD44 corresponding to 50,000 to 100,000 cpm. The time-corrected counts per minute (cpm) of the internalized fraction was converted into fmol based on the time-corrected specific activity, the MW of the scFv-Fc-CD44, and the efficacy of the gamma counter, and subsequently normalized to the number of tumor cells.

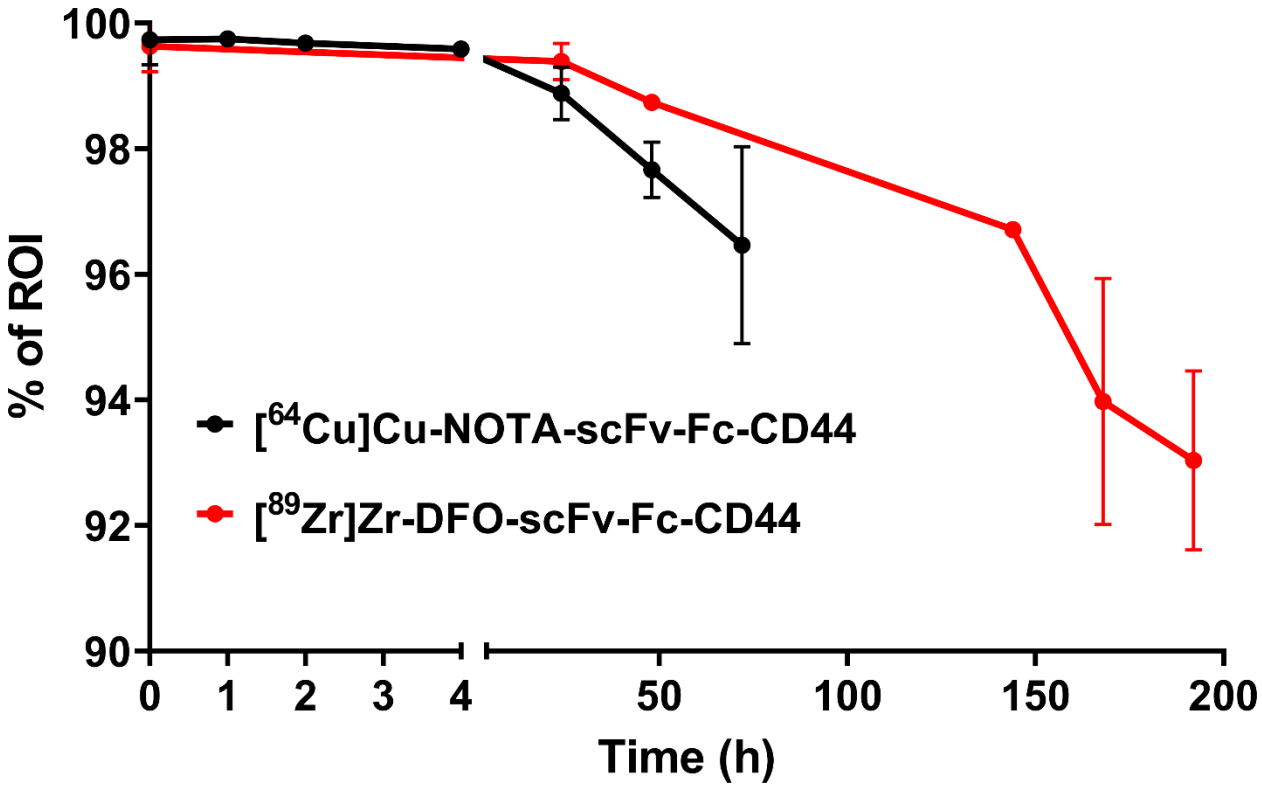

Supplemental Figure 13. ScFv-Fc-CD44 retained stable in human serum at 37° when conjugated and radiolabeled with [^{64}Cu]Cu-NOTA (black) or [^{89}Zr]Zr-DFO (red). The radiochemical purity (>99.5%) of the freshly radiolabeled constructs in PBS were first confirmed by ITLC representing the initial time point (0 h). To assess the stability *in vitro*, 2.7 MBq of the [^{64}Cu]Cu-NOTA-scFv-Fc-CD44 complex (74 µCi, 100 µl) was added to human serum (500 µl) in a microcentrifuge tube in triplicates and incubated at 37° while gently shaking at 300 rpm on an Eppendorf ThermoMixer. To the designated time points (1 h, 2 h, 4 h, 1 d, 2 d, and 3 d), 2 µl samples were withdrawn and evaluated by ITLC. Similarly, 2.0 MBq of the [^{89}Zr]Zr-DFO-scFv-Fc-CD44 complex (54 µCi, 100 µl) was incubated with human serum (500 µl) at 37° in triplicates, and 2 µl samples measured to later time points (1 d, 2 d, 6 d, 7 d, and 8 d) due to the longer half-life of ^{89}Zr compared to ^{64}Cu (78.4 h versus 12.7 h).

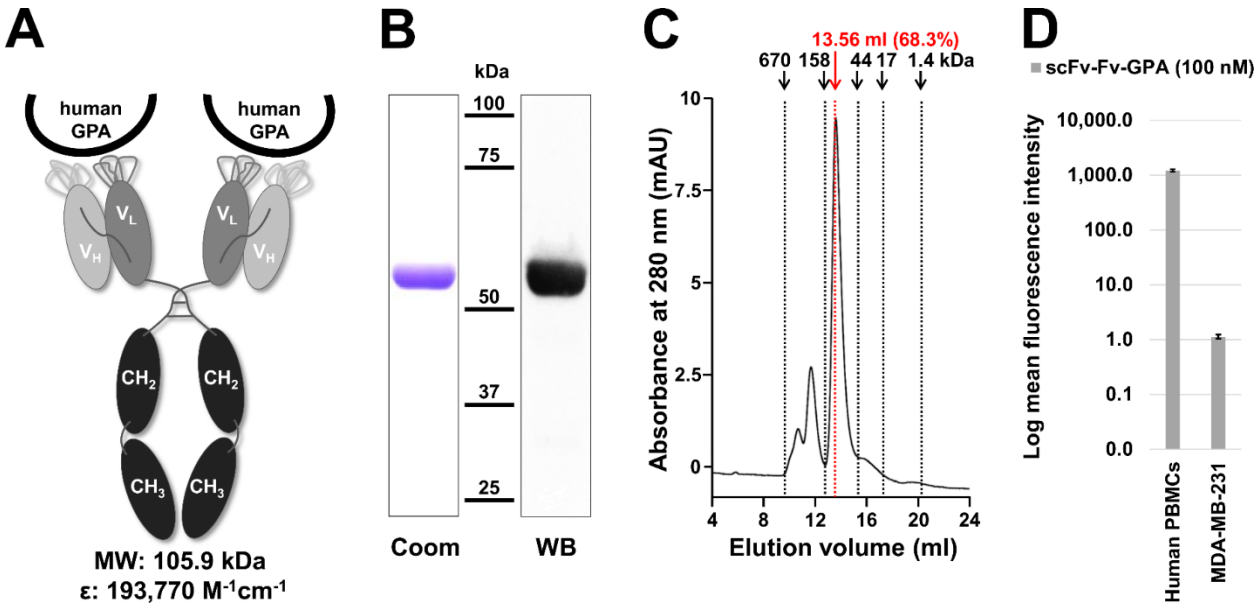

Supplemental Figure 14. Characterization of control scFv-Fc-GPA. The sequence of the variable domains was obtained from a hybridoma of parental mAb BRIC 256 (International Blood Group Reference Laboratory). The GPA binding site was cloned as scFv by connecting the VH and VL domain with an $(G_4S)_3$ linker, followed by sublconing into vector pYD11 (National Research Council of Canada) via NarI/EcoRV to add an C-terminal human IgG_1 Fc part. Plasmid DNA was transiently transfected into HEK293-6E cells and purified after five days of expression from supernatant via IMAC. (A) Based on the aa sequence, the theoretical MW was calculated to be 105.9 kDa with an extinction coefficient (ε) of 193,770 $M^{-1}cm^{-1}$ for the native scFv-Fc-GPA. (B) Characterization by Coomassie-stained gradient SDS-PAGE (5 µg/lane) of the reduced protein revealed high purity (>98%) with a distinct band for a reduced single-chain (theoretical MW: 52.95 kDa). The integrity was confirmed by WB using a goat anti-human pAb peroxidase conjugate (Jackson ImmunoResearch, #109-035-098). (C) Analysis of the oligomeric state of scFv-Fc-GPA (42 µg) by FPLC revealed a main peak of monomeric product (68.3% at 13.6 ml) and two smaller peaks corresponding to putative non-covalently linked dimers and trimers. (D) Flow cytometry confirms specific binding of the scFv-Fc-GPA to GPA expressed by human erythrocytes but not to MDA-MB-231 cancer cells. Detection was performed with a rabbit anti-human Fc fluorescein isothiocyanate conjugate (Jackson ImmunoResearch, #309-095-008). Data are represented as the mean of triplicates ±SE.

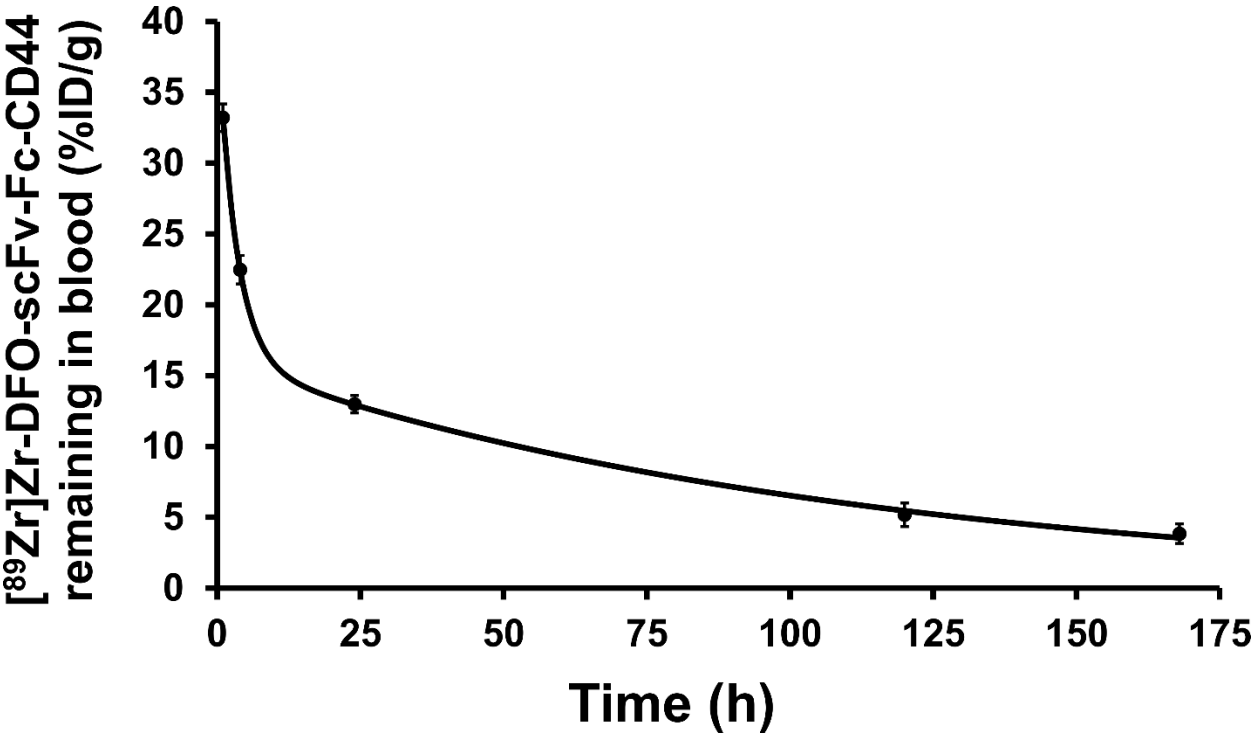

Supplemental Figure 15. *In vivo* blood clearance studies of the [^{89}Zr]Zr-DFO-scFv-Fc-CD44 in mice. Female CD-1 IGS mice (Charles River, strain 022) were intravenously injected with about 0.37 MBq (10 µCi) of [^{89}Zr]Zr-DFO-scFv-Fc-CD44 via the tail vein. After each time point (1 h, 4 h, 1 d, 5 d, and 7 d), blood was collected by small cheek bleeds. Each sample was weighed, and radioactivity counted with a Beckman Gamma-8000 counter. Blood uptake was calculated as percentage of injected dose per gram (%ID/g). Blood clearance parameter were analyzed by PKSolver 2.0 using the two-compartment analysis after IV bolus injection. Data represent the mean ±SE based on n=5 animals. According this analysis, $t_{1/2Alpha}$ (serum distribution half-life) of [^{89}Zr]Zr-DFO-scFv-Fc-CD44 in mice was 2.3 h and $t_{1/2Beta}$ (serum elimination half-life) was 77.2 h.

Supplemental Table 1. Biodistribution of [^{64}Cu]Cu-NOTA-scFv-Fc-CD44 in female NCI athymic NCr-nu/nu mice (Charles River, strain 553) with MDA-MB-231 tumor-xenografts at different time points (1 h, 4 h, and 24 h) post injection. Data are reported as the percent of the injected dose per gram of tissue (mean ±SE) based on five mice (n=5) per group.

Organ	1 hour	4 hours	24 hours
Tumor	3.3 ± 0.3	7.9 ± 1.5	22.7 ± 5.1
Blood	20.7 ± 1.7	14.1 ± 1.4	9.8 ± 0.3
Lung	9.5 ± 0.7	9.7 ± 0.9	6.5 ± 0.1
Liver	11.5 ± 0.5	12.8 ± 0.9	6.9 ± 0.4
Spleen	6.0 ± 0.6	7.4 ± 2.2	3.6 ± 0.1
Kidney	9.7 ± 0.6	11.3 ± 0.8	12.9 ± 1.3
Bladder	2.0 ± 0.1	4.9 ± 1.9	3.6 ± 0.3
Muscle	1.0 ± 0.1	1.5 ± 0.1	1.9 ± 0.1
Heart	5.6 ± 0.4	6.5 ± 0.4	4.2 ± 0.2
Bone	2.3 ± 0.3	3.1 ± 1.0	1.7 ± 0.1
Pancreas	2.1 ± 0.2	2.2 ± 0.2	2.0 ± 0.1
Stomach	0.9 ± 0.1	1.7 ± 0.3	1.4 ± 0.4

Supplemental Table 2. Biodistribution of [^{89}Zr]Zr-DFO-scFv-Fc-CD44 in female NCI athymic NCr-nu/nu mice (Charles River, strain 553) with MDA-MB-231 tumor-xenografts at different time points (1 d, 3 d, 5 d, and 7 d) post injection. Data are reported as the percent of the injected dose per gram of tissue (mean ±SE) based on four mice (n=4) per group.

Organ	1 day	3 days	5 days	7 days
Tumor	33.3 ± 6.4	43.9 ± 7.6	42.7 ± 6.9	55.5 ± 8.6
Blood	9.0 ± 2.3	6.3 ± 1.7	1.6 ± 0.7	2.3 ± 0.8
Lung	4.7 ± 0.8	4.4 ± 0.8	2.3 ± 0.2	2.6 ± 0.4
Liver	8.4 ± 2.4	7.2 ± 1.0	6.4 ± 0.3	7.1 ± 0.1
Spleen	7.9 ± 4.4	5.0 ± 0.9	4.4 ± 0.3	4.7 ± 0.7
Kidney	13.3 ± 1.2	15.0 ± 2.4	11.7 ± 1.6	15.1 ± 2.7
Bladder	3.7 ± 0.5	3.9 ± 0.3	2.3 ± 0.2	2.4 ± 0.2
Muscle	1.6 ± 0.3	1.4 ± 0.2	0.8 ± 0.1	0.7 ± 0.1
Heart	3.6 ± 0.5	2.9 ± 0.4	1.0 ± 0.1	1.3 ± 0.2
Bone	5.7 ± 2.4	9.0 ± 1.0	10.2 ± 1.6	11.9 ± 1.1
Pancreas	1.4 ± 0.1	1.3 ± 1.0	0.9 ± 0.0	0.9 ± 0.0
Stomach	0.9 ± 0.1	0.8 ± 0.1	0.4 ± 0.1	0.5 ± 0.1

Supplemental Table 3. Biodistribution of [^{64}Cu]Cu-NOTA-scFv-Fc-GPA (control) in female NCI athymic NCr-nu/nu mice (Charles River, strain 553) with MDA-MB-231 tumor-xenografts at different time points (4 h and 24 h) post injection. Data are reported as the percent of the injected dose per gram of tissue (mean ±SE) based on five mice (n=5) per group.

Organ	**4 hours**	**24 hours**
Tumor	4.6 ± 0.5	6.2 ± 0.8
Blood	13.5 ± 2.1	9.2 ± 0.6
Lung	5.6 ± 0.6	5.3 ± 0.3
Liver	18.9 ± 1.9	7.6 ± 0.7
Spleen	8.3 ± 2.5	3.6 ± 0.2
Kidney	7.2 ± 0.5	5.3 ± 0.4
Bladder	2.5 ± 0.5	3.6 ± 0.1
Muscle	1.2 ± 0.2	1.7 ± 0.1
Heart	4.7 ± 0.5	3.2 ± 0.2
Bone	2.8 ± 0.9	1.2 ± 0.1
Pancreas	1.5 ± 0.2	1.6 ± 0.1
Stomach	1.2 ± 0.1	0.8 ± 0.1

Supplemental Table 4. Biodistribution of [^{89}Zr]Zr-DFO-scFv-Fc-GPA (control) in female NCI athymic NCr-nu/nu mice (Charles River, strain 553) with MDA-MB-231 tumor-xenografts at different time points (1 d and 7 d) post injection. Data are reported as the percent of the injected dose per gram of tissue (mean ±SE) based on five mice (n=5) per group.

Organ	**1 day**			**7 days**		
Tumor	8.1	±	1.1	3.9	±	0.5
Blood	7.9	±	1.4	2.7	±	0.2
Lung	4.5	±	0.6	2.5	±	0.1
Liver	9.1	±	0.7	8.9	±	0.8
Spleen	5.9	±	0.9	4.3	±	0.4
Kidney	8.1	±	0.6	10.1	±	0.8
Bladder	3.5	±	0.3	2.3	±	0.1
Muscle	1.6	±	0.3	0.7	±	0.0
Heart	3.2	±	0.3	1.6	±	0.1
Bone	4.7	±	0.9	9.6	±	0.4
Pancreas	1.4	±	0.2	0.8	±	0.0
Stomach	1.0	±	0.0	0.4	±	0.0

Supplemental Table 5. Biodistribution of [^{89}Zr]Zr-DFO-scFv-Fc-CD44 in male NCI SCID/NCr mice (Charles River, strain 561) with PC3 tumor-xenografts at different time points (1 d and 7 d) post injection. Data are reported as the percent of the injected dose per gram of tissue (mean ±SE) based on five mice (n=5) per group.

Organ	**1 day**			**7 days**		
Tumor	20.7	±	2.5	31.9	±	3.1
Blood	16.0	±	0.6	5.3	±	0.1
Lung	8.2	±	0.5	5.0	±	0.1
Liver	7.2	±	0.3	7.9	±	0.4
Spleen	16.3	±	0.2	16.4	±	0.7
Kidney	10.0	±	0.4	8.4	±	0.2
Bladder	5.5	±	0.5	3.0	±	0.3
Muscle	2.6	±	0.1	1.0	±	0.0
Heart	6.3	±	0.4	2.7	±	0.1
Bone	6.4	±	0.3	12.8	±	1.0
Pancreas	2.4	±	0.1	1.3	±	0.0
Stomach	1.6	±	0.1	0.8	±	0.1

Supplemental Table 6. Biodistribution of [^{89}Zr]Zr-DFO-scFv-Fc-GPA in male NCI SCID/NCr mice (Charles River, strain 561) with PC3 tumor-xenografts at different time points (1 d and 7 d) post injection. Data are reported as the percent of the injected dose per gram of tissue (mean ±SE) based on five mice (n=5) per group.

Organ	**1 day**			**7 days**		
Tumor	6.0	±	0.3	3.5	±	0.1
Blood	14.9	±	0.4	4.5	±	0.1
Lung	8.4	±	0.4	4.7	±	0.1
Liver	10.3	±	0.4	11.2	±	0.4
Spleen	33.6	±	2.2	31.5	±	1.4
Kidney	6.4	±	0.4	6.8	±	0.2
Bladder	3.9	±	0.4	2.8	±	0.2
Muscle	2.1	±	0.1	1.1	±	0.1
Heart	6.0	±	0.3	2.7	±	0.1
Bone	9.7	±	0.4	19.7	±	1.7
Pancreas	2.3	±	0.0	1.3	±	0.0
Stomach	2.3	±	0.3	1.2	±	0.1

Supplemental Table 7. Tumor-to-organ ratios (TTOs) of the [^{64}Cu]Cu-NOTA-scFv-Fc-CD44 in female NCI athymic NCr-nu/nu mice (Charles River, strain 553) with MDA-MB-231 tumor-xenografts at different time points (1 h, 4 h, and 24 h) post injection. Tumor-organ ratios are averages of five mice (n=5) per group (mean ±SE).

Organ	**1 hours**			**4 hours**			**24 hours**		
Blood	0.2	±	0.0	0.6	±	0.1	2.3	±	0.6
Lung	0.4	±	0.0	0.9	±	0.2	3.5	±	0.8
Liver	0.3	±	0.0	0.6	±	0.1	3.4	±	0.1
Spleen	0.6	±	0.1	1.3	±	0.3	6.4	±	1.4
Kidney	0.3	±	0.0	0.7	±	0.1	1.9	±	0.6
Bladder	1.7	±	0.2	2.6	±	0.8	6.4	±	1.3
Muscle	3.3	±	0.3	5.4	±	1.1	12.1	±	3.1
Heart	0.6	±	0.1	1.2	±	0.2	5.6	±	1.5
Bone	1.5	±	0.2	3.2	±	0.9	14.3	±	4.5
Pancreas	1.6	±	0.1	3.7	±	0.7	11.3	±	2.6
Stomach	4.1	±	1.0	5.6	±	1.5	19.3	±	4.8

Supplemental Table 8. Tumor-to-organ ratios (TTOs) of the [^{89}Zr]Zr-DFO-scFv-Fc-CD44 in female NCI athymic NCr-nu/nu mice (Charles River, strain 553) with MDA-MB-231 tumor-xenografts at different time points (1 d, 3 d, 5 d, and 7 d) post injection. Tumor-organ ratios are averages of four mice (n=4) per group (mean ±SE).

Organ	1 day	3 days	5 days	7 days
Blood	4.5 ± 1.1	9.9 ± 3.2	39.4 ± 9.4	35.6 ± 11.0
Lung	7.2 ± 0.7	10.2 ± 0.6	18.8 ± 1.8	22.0 ± 1.6
Liver	5.1 ± 1.3	6.7 ± 1.5	6.7 ± 0.9	7.8 ± 1.0
Spleen	8.9 ± 2.8	10.3 ± 2.9	9.9 ± 1.8	13.1 ± 2.8
Kidney	2.5 ± 0.5	3.0 ± 0.3	3.6 ± 0.3	3.8 ± 0.4
Bladder	8.9 ± 1.1	11.2 ± 1.3	19.6 ± 4.0	22.9 ± 1.3
Muscle	21.0 ± 2.0	29.9 ± 1.9	51.8 ± 7.2	74.2 ± 5.9
Heart	9.2 ± 1.0	14.8 ± 0.7	41.2 ± 3.2	43.3 ± 4.4
Bone	9.1 ± 2.5	5.3 ± 1.2	4.4 ± 0.7	4.8 ± 0.7
Pancreas	23.2 ± 3.0	33.2 ± 4.9	48.6 ± 6.9	59.7 ± 9.7
Stomach	39.9 ± 9.3	53.5 ± 8.2	109.6 ± 17.6	151.0 ± 39.1

Supplemental Table 9. Tumor-to-organ ratios (TTOs) of the [^{64}Cu]Cu-NOTA-scFv-Fc-GPA control in NCI female athymic NCr-nu/nu mice (Charles River, strain 553) with MDA-MB-231 tumor-xenografts at different time points (4 h and 24 h) post injection. Tumor-organ ratios are averages of five mice (n=5) per group (mean ±SE).

Organ	**4 hours**	**24 hours**
Blood	0.4 ± 0.1	0.7 ± 0.1
Lung	0.8 ± 0.0	1.2 ± 0.2
Liver	0.3 ± 0.0	0.8 ± 0.1
Spleen	0.7 ± 0.1	1.8 ± 0.2
Kidney	0.7 ± 0.1	1.2 ± 0.1
Bladder	2.0 ± 0.2	1.7 ± 0.2
Muscle	4.0 ± 0.3	3.7 ± 0.6
Heart	1.0 ± 0.1	1.9 ± 0.2
Bone	2.2 ± 0.4	5.1 ± 0.5
Pancreas	3.3 ± 0.3	4.1 ± 0.5
Stomach	4.1 ± 0.5	8.0 ± 1.6

Supplemental Table 10. Tumor-to-organ ratios (TTOs) of the [^{89}Zr]Zr-DFO-scFv-Fc-GPA control in female NCI athymic NCr-nu/nu mice (Charles River, strain 553) with MDA-MB-231 tumor-xenografts at different time points (1 d and 7 d) post injection. Tumor-organ ratios are averages of five mice (n=5) per group (mean ±SE).

Organ	**1 day**	**7 days**
Blood	1.3 ± 0.3	1.4 ± 0.2
Lung	1.9 ± 0.3	1.6 ± 0.2
Liver	0.9 ± 0.1	0.5 ± 0.1
Spleen	1.5 ± 0.3	1.0 ± 0.2
Kidney	1.0 ± 0.1	0.4 ± 0.0
Bladder	2.3 ± 0.3	1.7 ± 0.2
Muscle	5.6 ± 1.1	5.4 ± 0.7
Heart	2.7 ± 0.5	2.5 ± 0.4
Bone	1.9 ± 0.4	0.4 ± 0.1
Pancreas	5.9 ± 0.9	4.6 ± 0.4
Stomach	8.0 ± 1.3	11.9 ± 2.4

Supplemental Table 11. Uptake ratios for specific ([^{64}Cu]Cu-NOTA-scFv-Fc-CD44) versus non-specific antibody ([^{64}Cu]Cu-NOTA-scFv-Fc-GPA) in NCI female athymic NCr-nu/nu mice (Charles River, strain 553) with MDA-MB-231 tumor-xenografts at different time points (4 h and 24 h) post injection. Ratios are based on the averages of five mice (n=5) per group.

Organ	**4 hours**	**24 hours**
Tumor	1.7	3.7
Blood	1.0	1.1
Lung	1.7	1.2
Liver	0.7	0.9
Spleen	0.9	1.0
Kidney	1.6	2.5
Bladder	1.9	1.0
Muscle	1.3	1.1
Heart	1.4	1.3
Bone	1.1	1.4
Pancreas	1.5	1.3
Stomach	1.5	1.7

Supplemental Table 12. Uptake ratios for specific ([^{89}Zr]Zr-DFO-scFv-Fc-CD44) versus non-specific antibody ([^{89}Zr]Zr-DFO-scFv-Fc-GPA) in NCI female athymic NCr-nu/nu mice (Charles River, strain 553) with MDA-MB-231 tumor-xenografts at different time points (1 d and 7 d) post injection. Ratios are based on the averages of four (n=4, [^{89}Zr]Zr-DFO-scFv-Fc-CD44) or five (n=5, [^{89}Zr]Zr-DFO-scFv-Fc-GPA) mice per group.

Organ	**1 day**	**7 days**
Tumor	4.1	14.3
Blood	1.1	0.8
Lung	1.0	1.0
Liver	0.9	0.8
Spleen	1.3	1.1
Kidney	1.6	1.5
Bladder	1.1	1.0
Muscle	1.0	1.0
Heart	1.1	0.8
Bone	1.2	1.2
Pancreas	1.0	1.1
Stomach	0.9	1.3

Supplemental Table 13. Mean and maximum standard uptake values (1 or 7 days post injection) of the [^{89}Zr]Zr-DFO-scFv-Fcs targeting CD44 or GPA (control) obtained from static PET imaging. Values were calculated from PET imaging with Inveon scanner from two pairs (n=2) of female NCI athymic NCr-nu/nu mice (Charles River, strain 553) and expressed as mean ±SE.

Organ	**1 day: CD44**	**7 day: CD44**	**1 day: GPA**	**7 day: GPA**
Tumor: SUV_{Mean}	8.5 ± 0.3	14.1 ± 1.0	4.00 ± 0.5	1.9 ± 0.3
Tumor: SUV_{Max}	12.2 ± 0.2	20.3 ± 2.1	5.6 ± 0.6	2.9 ± 0.5
Muscle: SUV_{Mean}	0.8 ± 0.1	0.3 ± 0.0	0.6 ± 0.3	0.2 ± 0.1
Muscle: SUV_{Max}	1.3 ± 0.2	0.8 ± 0.2	1.1 ± 0.1	0.7 ± 0.2